AgroLife Scientific Journal - Volume 3, Number 1, 2014
ISSN 2285-5718; ISSN CD-ROM 2285-5726; ISSN ONLINE 2286-0126; ISSN-L 2285-5718

NUMERICAL AND EXPERIMENTAL INVESTIGATIONS OF WIND LOADS ON PV SOLAR PANELS MOUNTED ON FLAT-ROOFS

Elena DRAGOMIRESCU, Ya LIU

University of Ottawa, 161 Louis Pasteur, K1G 5Y1, Ottawa, Canada, Phone: +1613.562.5800, Fax: + 1613.562.5173, Emails: Elena.Dragomirescu@uottawa.ca, yliu181@uottawa.ca

Corresponding author email: Elena.Dragomirescu@uottawa.ca

Abstract

As a vast renewable energy resource, solar energy is currently one of the most widely used types of new energy. For collecting solar energy devices based on photovoltaic (PV) cells are installed in locations with optimum exposure to sunlight. Wind-induced load is a main concern; however detailed guidelines and design codes for wind loads on PV solar panels are very limited. Therefore measurements were performed on a PV solar panel installed on the Mann Parking Building of the University of Ottawa. The wind load calculation was performed in conformity with the ASCE7-05 (2005) and SEAOC (2013) design codes, and it was noticed that the roof wind zone, building edge and the parapet effect were the main parameters affecting the estimated wind load value on each PV panel. The maximum wind load of 1,208.0 N was obtained on the northwest corner of the PV solar panel arrays, and the minimum wind load of 806.0 N was obtained on the centre of PV solar panel arrays.

Keywords*: wind-induced pressure, PV solar panels.*

INTRODUCTION

Exhaustible energy resources reduce gradually, even tend to depletion and over the years this issue became a main concern for sustainable development. Solar energy, as a vast and renewable energy resource, is currently one of the most employed measures of restoring the re-usable energy balance. The most common method of actively collecting the solar energy is represented by the photovoltaic (PV) solar cells which are installed on flat panels and these in turn are mounted on flat or inclined building roofs or at terrestrial level.

Several damages of PV solar panels or solar water heating systems installed on flat-roofs have been reported by Chung et al. (2007) for Taiwan region, where an average of 3.5 typhoons are recorded each year. Also a limited number of studies exist focusing on the structural analysis of the PV solar systems. Pfahl and Uhlemann (2011) studied the wind loads on heliostats and photovoltaic trackers at various Reynolds numbers (Re). They investigated the structure of a heliostat with 120 m^2 mirror area. Schellenberg (2013) studied the structural analysis and the application of wind loads on a solar arrays by the use of nonlinear wind induced response time history, which can account for some of the dynamic effects that would be captured by aeroelastic wind-tunnel testing. Aly (2013) studied the effects of model scale on ground-mounted solar panels. In this study, the authors investigated the sensitivity of wind loads to test ground-mounted solar panels, both in a boundary-layer wind tunnel and by using Computational Fluid Dynamics (CFD) simulation and they concluded that for the scaled models, the results from CFD simulations are more acceptable than the results obtained from the wind tunnel test. Numerical CFD simulations have also been attempted for small groups of PV solar panels by Hangan et al. (2008) and recommendations have been formulated regarding the angle of attack and the critical spacing between arrays of panels. Bitsuamlak et al. (2010) compared the results from numerical LES (Large Eddy Simulation) analysis with wind tunnel tests for ground mounted stand-alone and arrays of PV solar panels and they found very small differences, between the pressure coefficient distribution on the middle and side panel of each row. Radu et al. (1986) performed an experimental investigation on the steady wind pressures on

solar collectors mounted on flat-roofed medium-rise buildings. Their study was carried out in an open jet boundary-layer wind tunnel for a scaled model of a five-story rigid building of apartments supporting a roof with solar collectors mounted in simple and consecutive rows. Chung et al. (2010) carried out an experimental study in allow-speed wind tunnel, to investigate the mean surface pressure distributions and uplift force at different wind speeds, on solar collectors mounted on flat roofs of low rise buildings situated in typhoon prone regions. Also wind tunnel tests have been performed for singular PV panels (Hangan et al., 2008) or on three parallel arrays of PV panels (Shademan et al., 2009) and pressure distribution, drag and lift coefficients, overturning of middle panels and sheltering effect caused by the primary row of panels were investigated.

On-site measurements on PV solar panels are very difficult to obtain especially for the upper surface of the panels, because during their operation obstructing equipment cannot be installed on the upper surface bearing the silicon cells, as this might interfere with the collection of solar energy. Hence most of the real scale, on-site measurements are recorded for the back surface of the PV panels, or on the supporting frame, and by the aid of the formulations recommended by the designing codes, the wind force on the upper surface of the panel is determined.

Most of the National Building Codes do not have a specific chapter for the PV solar panels design guidelines, and it is understood that such structures should follow the cladding and other roof elements' static design criteria. However, technical design guidelines are under development worldwide, and these are to be used in conjunction with the national building codes available in the respective region or country. In California, US, interpretation of regulation document from the Division of the State Architect (DSA) is used as a resource by the DSA staff and design professionals to promote more uniform state wide criteria for designing the PV solar panels. DSA stipulates that PV solar panels and their balance-of-system must meet the wind force. A report was developed by the Structural Engineers Association of California's (SEAOC) Solar Photovoltaic System Committee which focuses solely on photovoltaic solar arrays on flat roof of low-rise buildings which includes the characteristics of wind flow on solar photovoltaic panels installed on the buildings`roof. Also for determining the gust factor and wind pressure coefficient (GCn) a figure is recommended for solar photovoltaic arrays on flat roof low-rise buildings determined based on the methodology contained in ASCE7-05 to determine the GCn value and the wind load for solar arrays installed on flat roofs.

EXPERIMENTAL SETUP AND THE PV SOLAR PANEL CONFIGURATION

The features of 180 watt maximum power poly-crystalline PV solar panel (Figure 1) are high conversion efficiency based on leading innovative photovoltaic technologies, and if properly installed it can withstand high wind-pressure, snow loads, and extreme temperature variations. The geometrical dimensions of one PV solar panel are 1.580×0.808×0.035 m (H×W×D). The PV solar panel is installed on a 2.10×0.83×1.40 m (H×W×L) frame which ensures a tilt angle of up to 35° (Figure 1).

Figure 1. PV Solar panel configuration and sensors layout

The instrumentation required for measuring the strain of the PV solar panel, which was used for calculating the stress and then the force acting at the specific points, is composed of a system of 7 uniaxial and 3 biaxial strain gauges, a AM16/32B multiplexer and a CR 1000 data logger. An anemometer and an external thermometer were also available at the site for collecting weather data. The PV solar panel is installed on the flat roof of Mann Parking

Building of the University of Ottawa. So far, most of the experiments presented in literature have replaced the PV solar panels with plywood, or plastic panels and they placed the sensors on the centre vertical and horizontal lines of the models, on both faces. The single case where a real PV solar panel was instrumented and strain gauges were placed on the front and back surfaces of the PV panel, in the limited space existing between the solar cells, is reported in the current project. A total of 13 strain gauges were placed in the centre cross lines as follows: on the vertical direction, three unidirectional strain gauges were placed at equal distance of about 26.8 cm starting from both ends and three bidirectional strain gauges (counting as double sensors, hence 6 unidirectional strain gauges) are placed in the 3 points in the middle; on the horizontal line two unidirectional strain gauges were installed near the edge of the PV panel. A similar configuration was used for the back side of the PV panel. The strain gauges are arranged as shown (Figure 1).

The temperature was measured every 2 minutes between the period of November 26, 2013 and December 10, 2013. The maximum registered temperatures were 8.8°C for the day of Dec 6, while the minimum temperature was recorded as -17.6°C for Dec 1. The variation of temperature for the given period was used for calibrating the signal recorded from the strain gauges.

Wind data was collected for the direction of the wind speed, maximum and average values (Figures 2 a, b) and for the intensity of the wind speed, minimum, maximum and average values, only the maximum values being reported in Figure 3. The North direction was considered as 0° angle for the wind speed direction. From measurements it was noticed that there were two main wind directions: the first wind direction was mostly between 340° and 350°, so it means that the wind speed approached the PV panel from the northwest direction. The second dominant wind direction was mostly between 100° and 150°, which is equivalent to the wind speed approaching the PV panel from the southeast direction. The PV solar panel orientation installed on the flat roof was set as north-south.

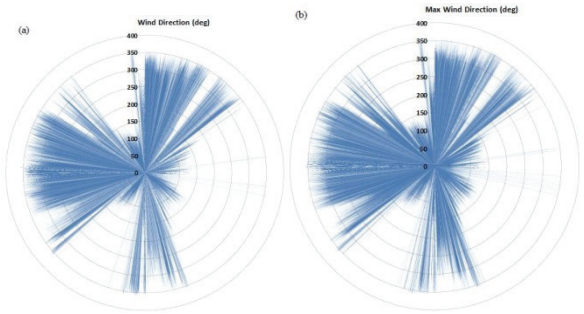

Figure 2. Wind speed direction for the Nov-Dec 2013 period: a) average values, b) maximum values

The wind speed intensity for the Nov-Dec 2013 period varied between the highest values of 7.9 m/s on Nov 28, 8.0 m/s on Dec 5, 8.9 m/s on Dec 10 and lowest values of 0 m/s. The negative values of the wind speed are considered as positive values, but for a different wind direction, hence the data doesn't contain values below the x axis. Also because the critical response of the PV solar panel was of interest, the focus was mainly on the maximum recorded values.

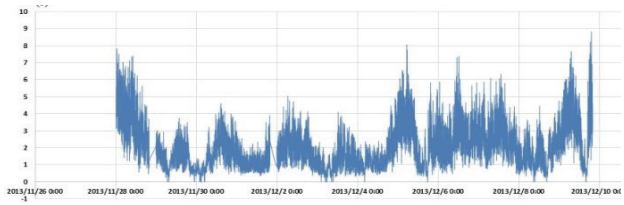

Figure 3. Maximum wind speed direction for the Nov-Dec 2013 period

MEASUREMENTS RESULTS

Calibration of data was required in order to account for several factors, such as temperature effect upon the length of the wire, resistance induced by the lead wire and the gauge factor induced by the sensor - wire attachments. The influence of temperature variation of lead wires is represented by:

$$\varepsilon l = \frac{r \cdot L \cdot \alpha \cdot \Delta T}{K(R + r \cdot L)} \qquad (1)$$

Where εl is thermal output of lead wires,r istotal resistance per meter of lead wires (Ω/m), $L$is the length of lead wires (m), α represents the temperature coefficient of resistance of lead wires (copper wire $3.9\times10^{-}$

$^{3}/℃$ is used), ΔT istemperature variation, K is the gauge factor and R is the gauge resistance. Also the gauge factor correction due to the lead wire attachment was determined by:

$$K_0 = \frac{R}{R + \frac{r \cdot L}{2}} \cdot K \qquad (2)$$

Where K_0 is thecorrected gauge factor.
Sensors were placed on the vertical and horizontal centrelines of the PV solar panel on both front and back surfaces. Three biaxial sensors were used for the middle points of the vertical line, in order to capture the stress in both transversal and longitudinal direction. The upper and lower edges were also instrumented each with 3 uniaxial strain gauge sensors; however the sensors at the superior part of the panel were lost due to harsh winter conditions. For each face of the PV solar panel a total of 13 sensors (7 uniaxial strain gauges and 3 biaxial strain gauges, each counting as a double sensor) remained in place (Figure 4). The strain data collected directly from the uniaxial and from the biaxial strain gauges cannot be interpreted directly and it must be converted into stress.

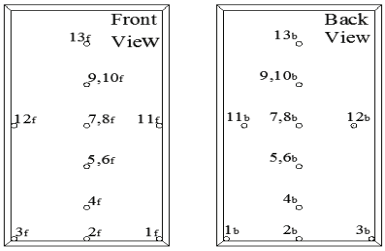

Figure 4. Strain gauges sensors location

Figure 5 shows the distribution of stress on the front surface of the PV Solar Panel. It illustrates that sensor 1, located at the lower corner of the PV panel, has the highest maximum stress and minimum stress, hence the highest stress variation; rather, sensor 7, at the middle of the PV panel has the lowest maximum stress and minimum stress. Also was noticed that the stresses recorded by sensor 2 are slightly higher than the ones from sensor 3, both located on the lower horizontal line of the PV panel. The stresses from sensor 4 and sensor 13, along the vertical line, near the lower and upper edges of the PV panel respectively, are the highest when compared with the rest of the sensors. The maximum stress on sensor 11 is very close to sensors 4 and 13. The stresses on sensor 5 and 6 are larger than sensor 9 and 10. Sensor 8 and sensor 9 almost have the same stresses

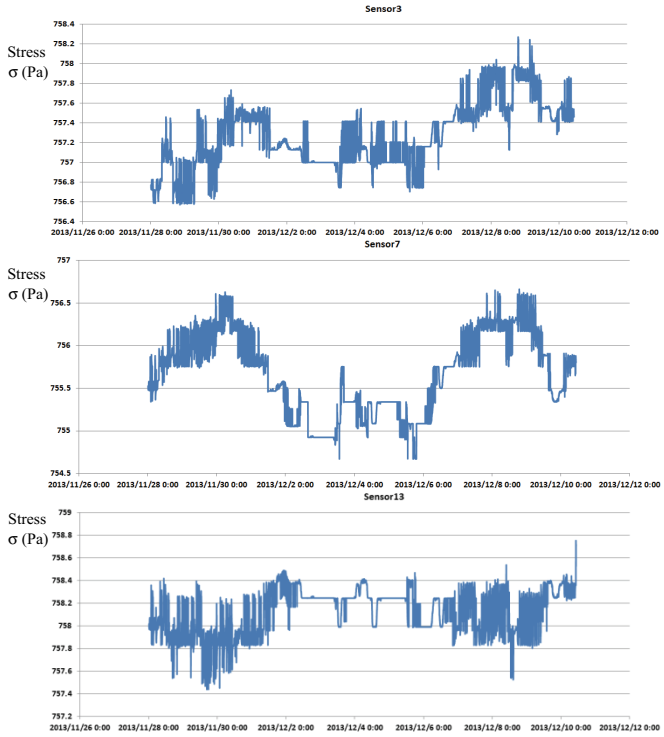

Figure 5. Stress data at selected locations on the front surface of the PV panel

Figure 6 shows the stress distribution on back surface of the PV solar panel; there are is some discrepancy between the results measured on the two surfaces. Sensor 7 in the middle of the panel has the highest values for maximum and minimum stress; rather, sensor 1, on the horizontal line, near the lower edge of the panel, has the lowest maximum stress and minimum stress. The stresses recorded by sensor 3 are slightly higher than the stresses from sensor 2, both located on the lower edge of the panel, in the corner and in the middle of the horizontal line, respectively. The stresses on sensor 4 and sensor 13, located on the vertical line, on both sides of the middle point of the panel, have the lowest stresses when compared with the rest of the sensors. The maximum stress measured on sensor 12 is very close to the stress on sensor 11, both on the middle horizontal line, near the lateral edges of the panel.

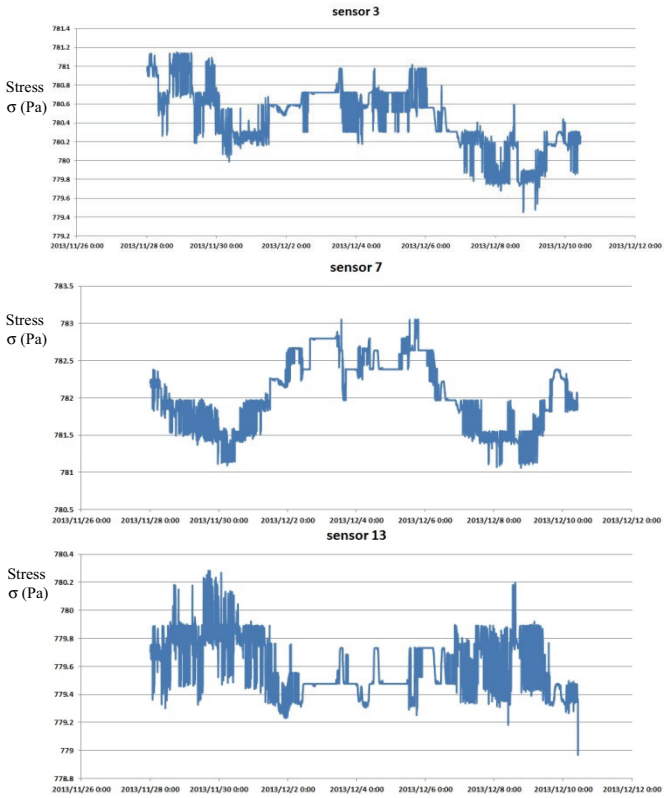

Figure 6. Stress data at selected locations on the back surface of the PV panel

The stresses on sensor 5 and 6 (biaxial sensor), on the vertical middle line, representing stresses on both longitudinal and transversal axes of the panel, are lower than the stresses from sensor 9 and 10 representing stresses on the same two directions, but on the superior part of the vertical line. Sensor 8 and sensor 9 still have almost the same stresses.

(a)	53.82	
	53.74	
53.76	53.70	53.78
	53.77	
	53.83	
53.78	53.80	53.91

(b)	55.35	
	55.44	
55.40	55.48	55.42
	55.41	
	55.35	
55.27	55.38	55.40

Figure 7. Distribution of average force (N) on the PV solar panela) front surface b) back surface

In order to investigate the distribution of force on both sides, the panel is divided in 18 equal patches on which the sensors are placed and these are considered as the sensor(s) as tributary area. The area of each patch is $0.071 m^2$. The average forces on every patch are shown in Figure 7 while the sensors' location is shown in Figure 4. For the areas where no forces are shown, no sensor was placed, or the sensors were lost due to the weather conditions. The average force on the front surface of PV solar panel 967.207 N and the average force on the back surface of PV solar panel was 996.465 N.

DESIGN CODE RECOMMENDATIONS FOR PV SOLAR PANELS

The current project focused on instrumenting and measuring the wind-induced pressures and forces for a singular PV solar panel, results which will be used for calibrating larger models and bigger cluster arrangements of PV solar panels. It is not probable to have installation of such stand-alone panels for current applications; hence the design guidelines always provide the recommendation for multiple arrays of PV solar panels.

The SEAOC (2013) design specifications divide the roof into 3 zones: interior zone, edge zone, and corner zone. If solar panels are mounted on the roof, the corner zones have much higher wind induced pressure than on the roof itself. As the height above the roof or length of the module increases, the wind loads increase. In order to make the figure fit most solar photovoltaic installations, the maximum height above the roof surface (h2) for solar modules should be limited to 4 feet and the length (lp) should be limited to 6 feet 8 inches; the height of the gap between the modules and the roof surface (h1) should not exceed 2 feet to prevent creation of excessive uplift. A reduction factor, γc (0.8~1.0), is used for reducing the wind loads for shorter modules, which applies only to the higher tilt angle (ω = 15° to 35°). If there are parapets on the roof, it worsens the wind loads on solar modules, so that the codes limit the parapet height to 4 feet unless the GCn values are increased by a 1.3 factor. For considering low-rise buildings, ASCE7-05 reports standardized graphs representing the wind pressure coefficients GCn as function of the normalized wind area which is different than the effective wind area. 15 feet is set as a lower limit on the height of building, and GCn values are not limited at

normalized wind areas of less than 1. According to the wind tunnel data, there is not a linear relationship between the GCn values and the panel tilt angle over the full tilt angle range. Hence two GCn curves are created to illustrate the phenomenon. There is a small change in GCn values for lower tilt modules in the 1° to 5° range and for higher tilt modules in the 15° to 35° range.

The calculation of the wind induced forces performed considering several scenarios of a single PV panel placed in the following locations as shown in Figure 8.

Location 1: panel is located in Zone 3 of the roof and in the centre of the PV panel array.

Location 2: panel is located in Zone 3 of the roof and in the Northeast corner of the PV panel array.

Location 3: panel is located in Zone 3 of the roof and in the Northwest corner of the PV panel array.

Location 4: Panel is located in Zone 2 of the roof and in the Southwest corner of the PV panel array.

Location 5: Panel is located in Zone 2 of the roof and in the Southeast corner of the PV panel array.

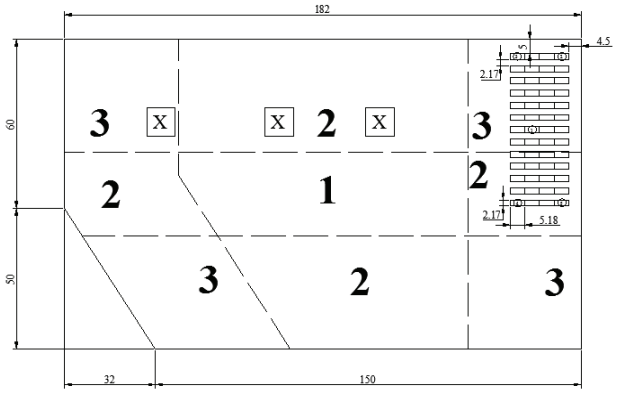

Figure 8. PV panels location on the flat-roof (SEAOC, 2013)

To convert the allowable stress design wind loads to the ASCE7-05 Design Code, multiplying the estimated wind loads by a safety factor of 0.6 was considered. The calculation was carried out in imperial unit systems, because some of the non-dimensional factors recommended in the ASCE7-05 code are applicable only to the ft-lb unit systems. Final values are converted to the international unit system.

The PV panels' array geometry and the building dimensions are considered within the limits recommended by the ASCE7-05 hence the required minimum air gaps around each PV module are provided. Also the dimensional requirement is fulfilled since none of the arrays of PV panels are closer than 4 feet from any roof edge. The area for the PV panel was determined as:

$$a_{pv} = 0.5\sqrt{hw_L} \quad (4)$$

If the value of a_{pv} is higher than h, then a maximum value of 20 feet should be used, a_{pv} = 30 feet was determined in the current study therefore in the calculation $_{pv}$ = 20 feet was used. For determining the roof zones where the panels are located, the condition of $2a_{pv}$=40ft is considered for roof zone 2 and 3 setbacks. Panels located beyond 40 ft setback are in roof zone 1. For the current study, roof zone 0 is applicable, since no condition exists where a setback is higher than $5a_{pv}$=100 feet.

The average load distributed along the panel will be transferred to the fasteners connecting the panel to the frame. The effective wind area (A) estimated for each of a module fastener is:

$$A = \frac{1}{4} \times l_p W_{module} \quad (5)$$

For selecting the pressure coefficient GCn as recommended by the ASCE7-05, design code, the normalized wind speed area was determined as:

$$A_n = \left(\frac{1000}{\left(\max\left(a_{pv}, 15\ \text{ft}\right)\right)^2} \right) \quad (6)$$

The pressure coefficient for each roof zone were read from the tables provided in ASCE7-05, based on A = 3.23 feet^2, An = 8.0 and are represented in Table 1.

Table 1. Pressure coefficient GCn

Roof Zone	0°~15°	15°~35°	(15°~35°)*γc
1	1.12	1.52	1.38
2	1.48	2.15	1.95
3	1.70	2.60	2.36

The chord length adjustment factor (γc) for the GCnat higher tilt angles of 15°≤ω≤35° is obtained by interpolating γc = 0.6+0.06 × lp =0.6+0.06×(5.18 ft^2). The interpolation results for all the roof zones are detailed in Table 2.

Table 2. Chord length adjustment factor (γc)

ω	A_n	Roof Zone		
		3	2	1
0°~15°	1-500	-0.66log(A_n)+2.3	-0.57log(A_n)+2.0	-0.42log(A_n)+1.5
0°~15°	500-5000	-0.35log(A_n)+1.44	-0.3log(A_n)+1.26	-0.25log(A_n)+1.0
15°~35°	1-500	-1.0log(A_n)+3.50	-0.83log(A_n)+2.90	-0.53log(A_n)+2.0
15°~35°	500-5000	-0.3log(A_n)+1.61	-0.25log(A_n)+1.3	-0.25log(A_n)+1.2

The edge factor (E) was determined considering the characteristic height:

$$h_c = \min(h_1, 1ft) + l_p \sin\omega \quad (7)$$

Where h_c = 3.09 feet, except when evaluating a panel toward a building edge unobstructed by panels, then $h_c = 0.1a_{pv}$. Also h_c = 2.0 feet when evaluating E for a building roof with PV panels unobstructed by the edge. The parapet height factor (γ_p) was considered γ_p =1.0, since h_{pt}<4 feet. The calculation of GC_n is provided in Table 3 for different locations of the PV panel inside the array and for the corresponding roof regions.

To complete the calculation of the maximum wind load on each PV module fastener to the supporting racking system, the wind velocity pressure (q_h) must be determined based on the ASCE 7-05, Equation 29.3-1:

$$q_h = 0.00256 K_z K_{zt} K_d V^2 \quad (8)$$

Where the exposure coefficient at 20 feet was K_z= 0.9 (ASCE 7-05), K_{zt} = 1.0, K_d = 0.85 (ASCE 7-05, Table 2 6.6-1). For a wind speed corresponding to Ottawa region of V = 110 mph, a velocity pressure of q_h = 23.70 lbs/ft^2 was determined.

As per the calculation of the final forces presented in Table 3, was noticed that the Location 3 has the maximum net pressure coefficient, and LRFD pressure value and the maximum wind load 1.208 N is acting on it. Location 4 and 5 have the same edge factor, net pressure coefficient, and LRFD pressure value and wind load. All the forces and net pressure coefficients of Location 2 are very close to the ones from Location 4 and 5.

Table 3. The Calculation of (GCn) net values and The Maximum Wind Load on Each Panel

Loc	E	Roof Zone	GCn*γ_c	$(GCn)_{net}$ =γ_pE(GCn*γ_c)	p=$q_h(GCn)_{net}$		F=P*A (N) LRFD
					LRFD (N/m^2)	(ASD) (N/m^2)	
1	1	3	2.36	2.36	56	34	806
2	1.13	3	2.36	2.67	63	38	910
3	1.5	3	2.36	3.54	84	50	1208
4	1.5	2	1.95	2.925	69	42	998
5	1.5	2	1.95	2.925	69	42	998

Location 1 had the minimum net pressure coefficient, LRFD pressure value and the minimum wind load of 806 N acting on the PV panel.

CONCLUSIONS

Based on the calculation procedure recommended by the SEAOC (2013) design code, the maximum wind load on the PV solar panels mounted on the flat roofs is obtained based on a method similar to that contained in ASCE7-05. From the calculation performed in the current study, there are two main parameters to influence the value of wind load on each PV panel, namely the roof zone and the building edge with parapet effect. The sheltering effect is significant on Location 1 which is in the centre of the array.

From the on-site measurements performed on a singular panel installed on the roof of Mann Parking Building at University of Ottawa, the highest wind - induced stresses are on the lower edge of the PV panel and the lowest stresses are on middle point of the front surface of the PV solar panel; however, for the back surface of the PV panel the opposite situation was noticed, the highest stresses are in the middle of the panel, and the lowest stresses are on the lower edge of the back surface of the PV solar panel. In general, for the front surface, the sensors which are on the edge of PV solar panel are subjected to higher stresses than the sensors on the centre of PV solar panel; rather, the sensors on edge of the back surface are

sheltered by the frame so that the stresses acting on them are lower than the sensor which are on the centre lines.

The average force on the experimental PV solar panel is very close to the average force on the location 4 and 5 determined as per the design code recommendations; however, these are not in the same roof zone. The experimental PV panel and the location 2 have the same position on each roof. Both of them are in zone 3 which is the corner of roof and next to the parapets, and the average force on location 2 is 910 N which is slightly smaller than the experimental one. This shows that the zone of the roof and the parapets affect the estimation of the wind load on the solar panel.

ACKNOWLEDGEMENTS

This research work was carried out with the support of Natural Sciences and Engineering Research Council of Canada. Also the assistance of Dr Karin Hinzer and the entire SunLab Research Team, who allowed us to perform measurements on their PV solar panels and to use the collecting data system, is greatly acknowledged.

REFERENCES

Aly M., Bitsuamlak G., 2013. Aerodynamics of ground-mounted solar panels: Test model scale effects, in Proc. of The 13 American Wind Eng. Conf., Seattle, USA.

ASCE 7-05, 2005. Chapter C6 wind loads.

Bitsuamlak G.T., Dagnew A.K., and Erwin J., 2010. Evaluation of wind loads on solar panel modules using CFD. In Proc. of The Fifth International Symposium on Computational Wind Engineering, Chapel Hill, North Carolina, USA, May, p. 23-27.

California Structural Engineers Association, 2013. Wind Design for Low-profile Solar Photovoltaic Arrays on Flat Roofs.

Chung K., Chang K., Liu Y., 2008. Reduction of wind uplift of a solar collector model. Journal of Wind Eng. and Ind. Aerod., Vol. 96, p. 1294-1306.

Chung K., Chang, K., Liu Y., 2008. Reduction of wind uplift of a solar collector model. Taiwan.

Chung Keh-Chin Chang, Chin-Cheng Chou, 2010. Wind loads on residential and large scale solar collector models.

Hangan H., 2010. A study of wind effects for solar power products panel mount system. Report BLWT-SS8-2010, Alan G. Davenport Wind Engineering Group.

Maffei J., Telleen K., Ward R., 2012. Wind Design Practice and Recommendations for Solar Arrays on Low-Slope Roofs.

Pfahl A., Uhlemann H., 2011. Wind loads on heliostats and photovoltaic trackers at various Reynolds numbers. Journal of Wind Eng. and Ind. Aerod., Vol. 99, p. 964-968.

Pratt R.N., 2012. Wind Field Measurements Around Photovoltaic Panel Arrays Mounted on Large Flat-roofs.

Radu A., Axinte E., and Theohari C., 1986. Steady wind pressures on solar collectors on flat-roofed buildings.

SEAOC, 2013. Solar Photovoltaic Systems, Wind design for low-profile solar photovoltaic arrays on flat roofs.

Schellenberg A., Maffei J. and Tell K., 2013. Structural analysis and application of wind loads to solar arrays. Jornal of Wind Eng. and Ind. Aero. (in Press).

Shademan M., Hangan H., 2009. Wind Loading on Solar Panels at Different Inclination Angles. in Proceedings of 11th Americas Conference on Wind Engineering, San Juan, Puerto Rico.

Shademan M. and Hangan H., 2010. Wind loading on solar panels at different azimuthal and inclination angles. in Proc. of The Fifth International Symposium on Computational Wind Engineering, Chapel Hill, North Carolina, USA, May, p. 23-27.

Wang Ying-Ge, Li Zheng-Nong, Gong Bo, Li Qiu-Sheng, 2008. Time-domain analysis on wind-induced dynamic response of heliostat.